Supporting Information

Role of pH Controlled DNA Secondary Structures in the Reversible Dispersion/Precipitation and Separation of Metallic and Semiconducting Single-walled Carbon Nanotubes

Basudeb Maji,[a] Suman K. Samanta,[a,#] Santanu Bhattacharya*[a,b,c]

[a]*Department of Organic Chemistry, Indian Institute of Science, Bangalore 560012, India.*

Fax: +91-80-23600529; Tel: +91-80-22932664; E-mail: sb@orgchem.iisc.ernet.in

[b]*Jawaharlal Nehru Centre for Advanced Scientific Research Bangalore 560064, India.*

[c]*J. C. Bose Fellow, Department of Science and Technology, New Delhi, India.*

[#]*Present address: Makromolekulare Chemie, Bergische Universitat Wuppertal, Gaussstrasse 20, 42119 Wuppertal, Germany.*

Corresponding author. E-mail addresses

sb@orgchem.iisc.ernet.in (S. Bhattacharya)

Table of contents.

Purification of the HiPco SWNTs

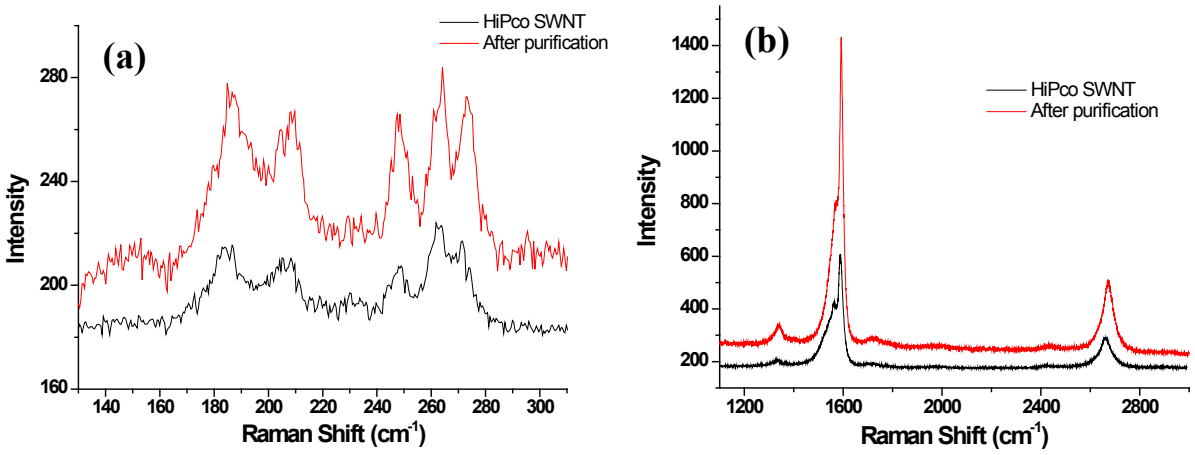

Figure S1. Raman spectra of SWNT before and after purification (a) RBM region and (b) G and 2D band.[I]

Additional UV-Vis-NIR spectra of the DNA and DNA-SWNT complex

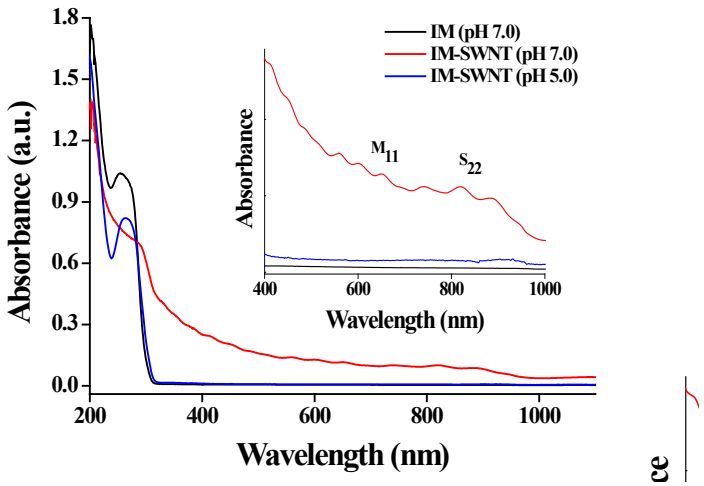

Figure S2. (a) Absorption spectra of IM and IM-SWNT hybrid at different pH, inset showing magnified spectra at 400-1000 nm. Corresponding absorption bands of M_{11} and S_{22} disappeared at pH 5 indicating that the SWNTs were absent in the acidified solution.

Zeta potential measurement

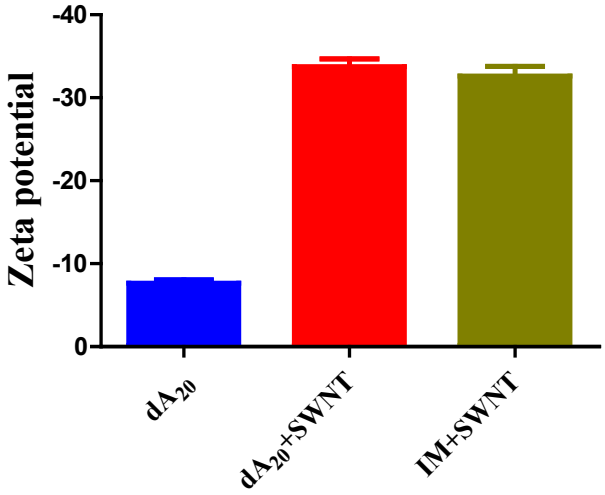

Figure S3. Zeta potential plot of DNA and DNA-SWNT hybrids in deionized water. [DNA] = 10 μM in each case.

Addditional AFM images

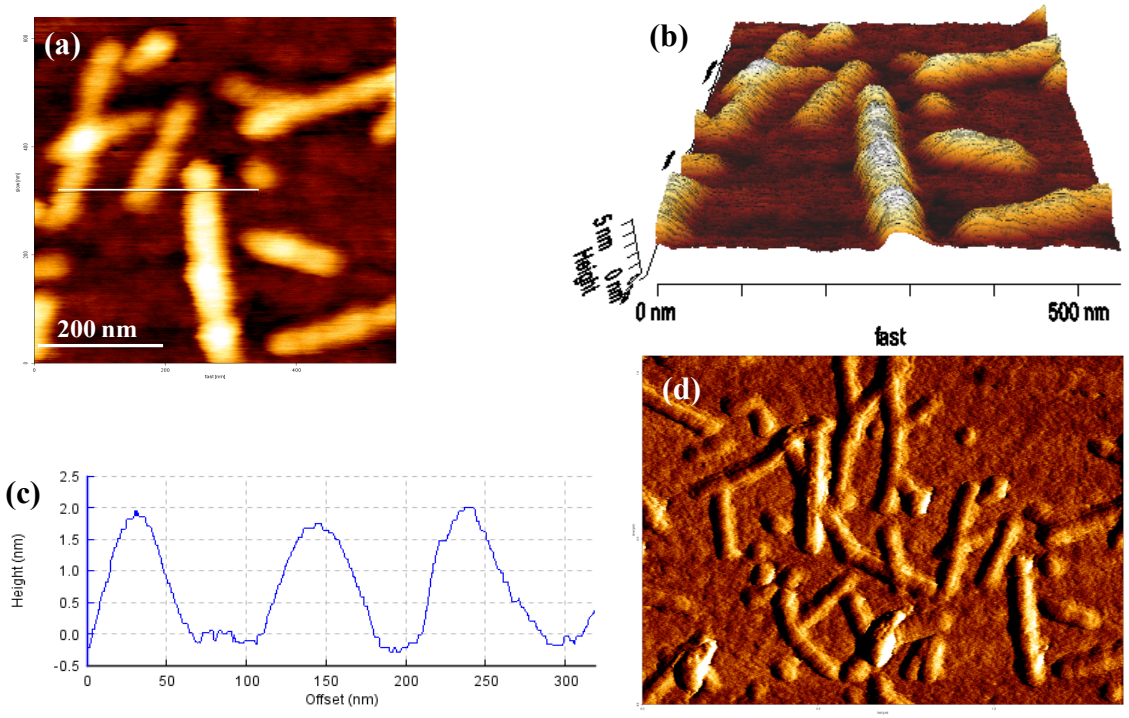

Figure S4. (a) AFM images of dA_{20}-SWNT complexes and (c) corresponding height profile, (b) 3D image profile of the dA_{20}-SWNT complexes. (D) Amplitude image of dA_{20}-SWNT complexes.

Addditional AFM images

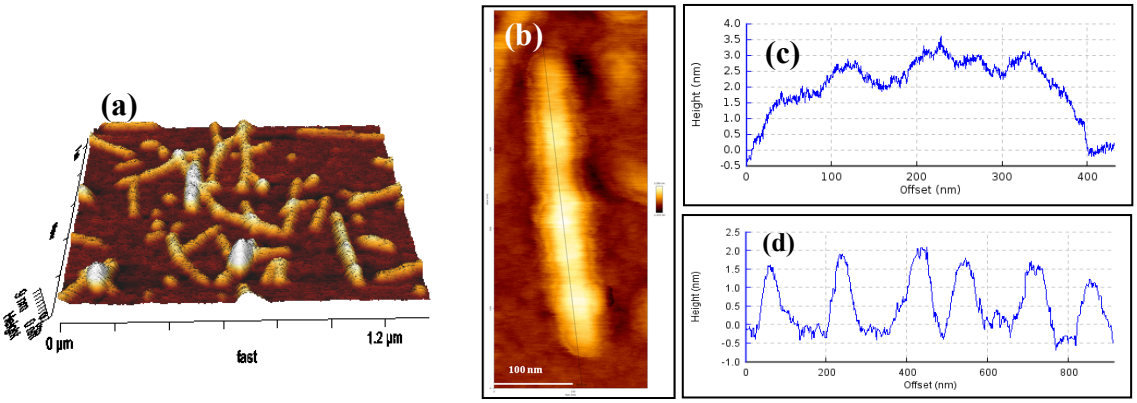

Figure S5. (a) AFM images of dA_{20}-SWNT complex showing individual SWNTs and (d) corresponding height profile. (b) AFM height image of single IM-SWNT complex and (c) corresponding surface height profile.

Base pairing in A/i-motif DNA

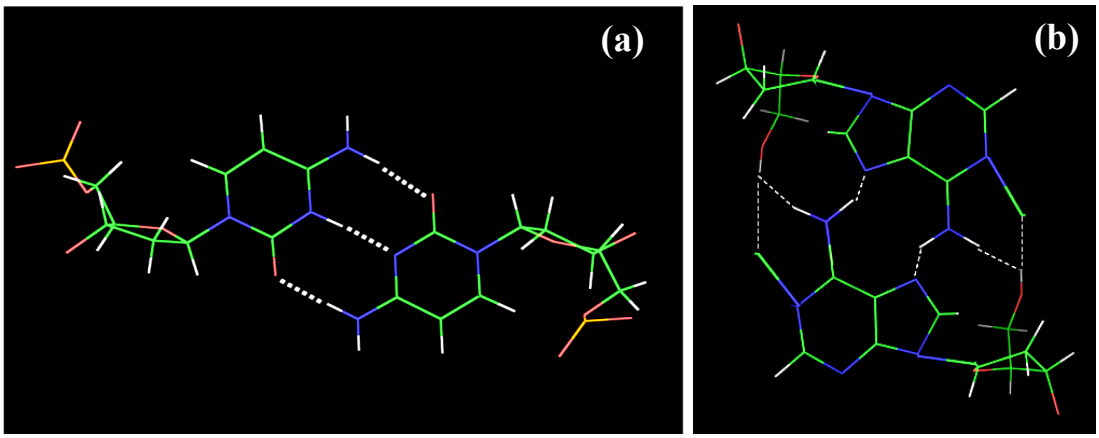

Figure S6. Base pairing scheme in (a) C-C^+ between the protonated and non-protonated cytosines[II] and (b) AH^+-H^+A through the protonated adenosines.[III]

Role of dT_{20} in the dispersion of SWNTs at different pH

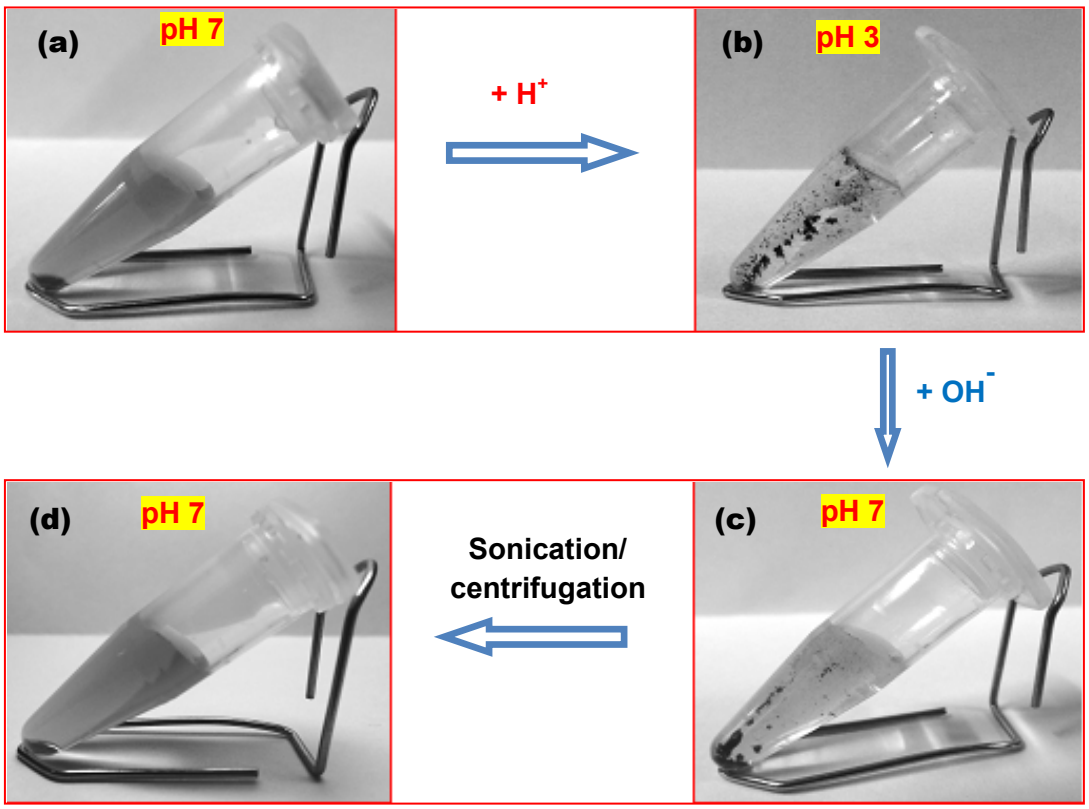

Figure S7. Effect of pH variation on the dT_{20}-SWNT complex dispersion in aqueous medium. (a) dT_{20}-SWNT at pH 7.0; (b) dT_{20}-SWNT at pH 3.0; (c) basification of the sample **b** containing dT_{20}-SWNT to pH 7.0 and (d) Sample **c** redispersed after a brief sonication at pH 7.0.

Ionization of different nucleobases at different pH

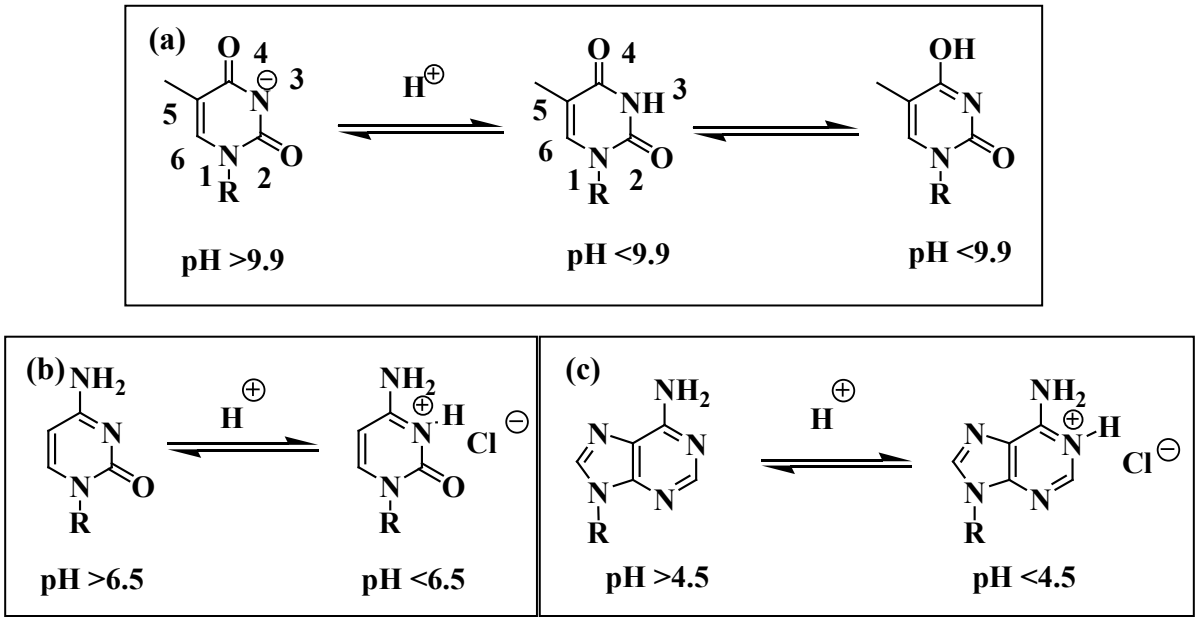

Figure S8. Ionization of different nucleobases in the nucleotide (a) thymine, (b) cytosine and (c) adenine at different pH.

The presence of dT_{20} along with dA_{20} generated a duplex DNA (Watson-Crick) structure (Figure S9b) which was found to be inefficient in dispersing SWNT in water. This observation suggests that duplex DNA formation is more favorable than the single-stranded DNA induced SWNT complexation. This is consistent with earlier report.[IV]

Effect of pH variation on the dT_{20}-SWNT complex

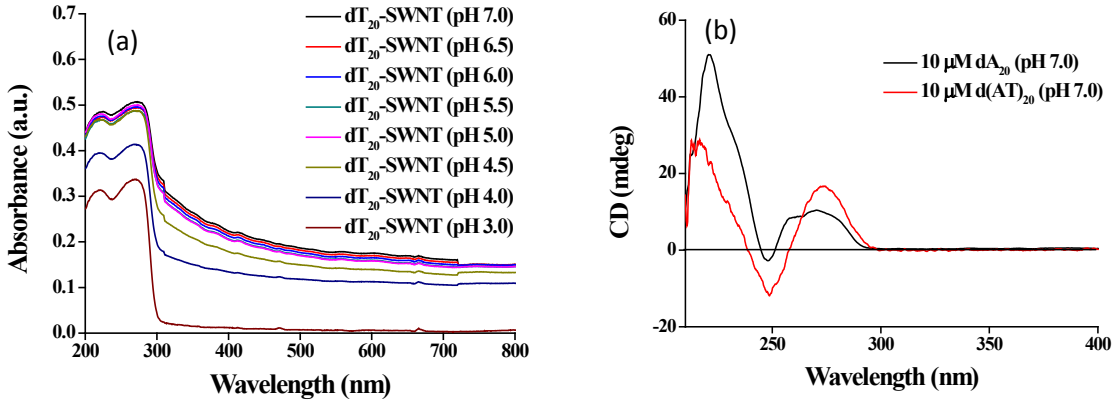

Figure S9. (a) Effect of pH to the dT_{20}-SWNT dispersion probed by UV-Vis-NIR spectroscopy. (b) CD signatures of dA_{20} and $d(A_{20}\cdot T_{20})$ duplex DNA at pH 7.0.

Determination of p*K*a values

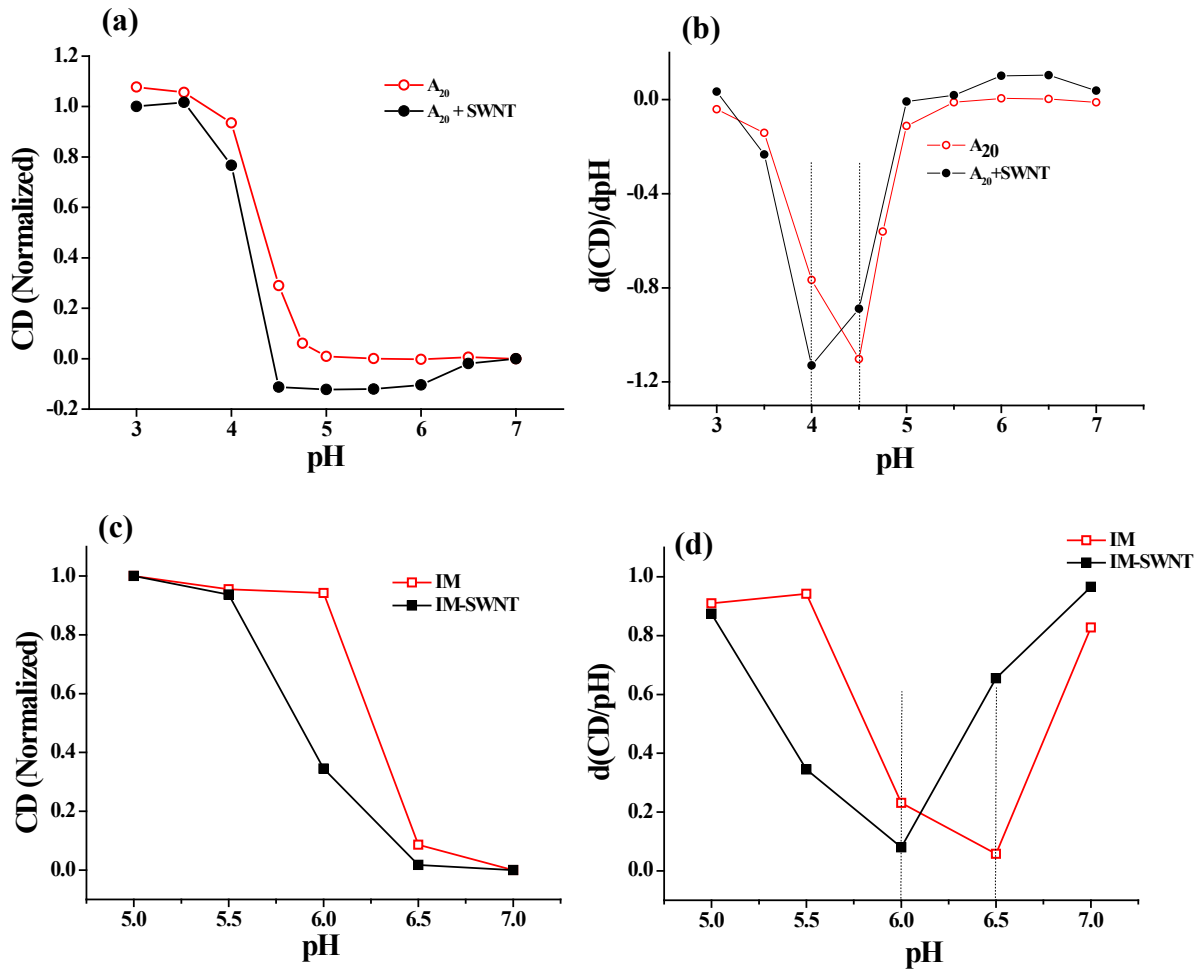

Figure S10. Plot of CD intensity of (a) dA_{20} and dA_{20}-SWNT and (c) IM and IM-SWNT as a function of pH. (b, d) are the corresponding first-derivative plots respectively.

Thermal stability of DNA and DNA-SWNT complexes

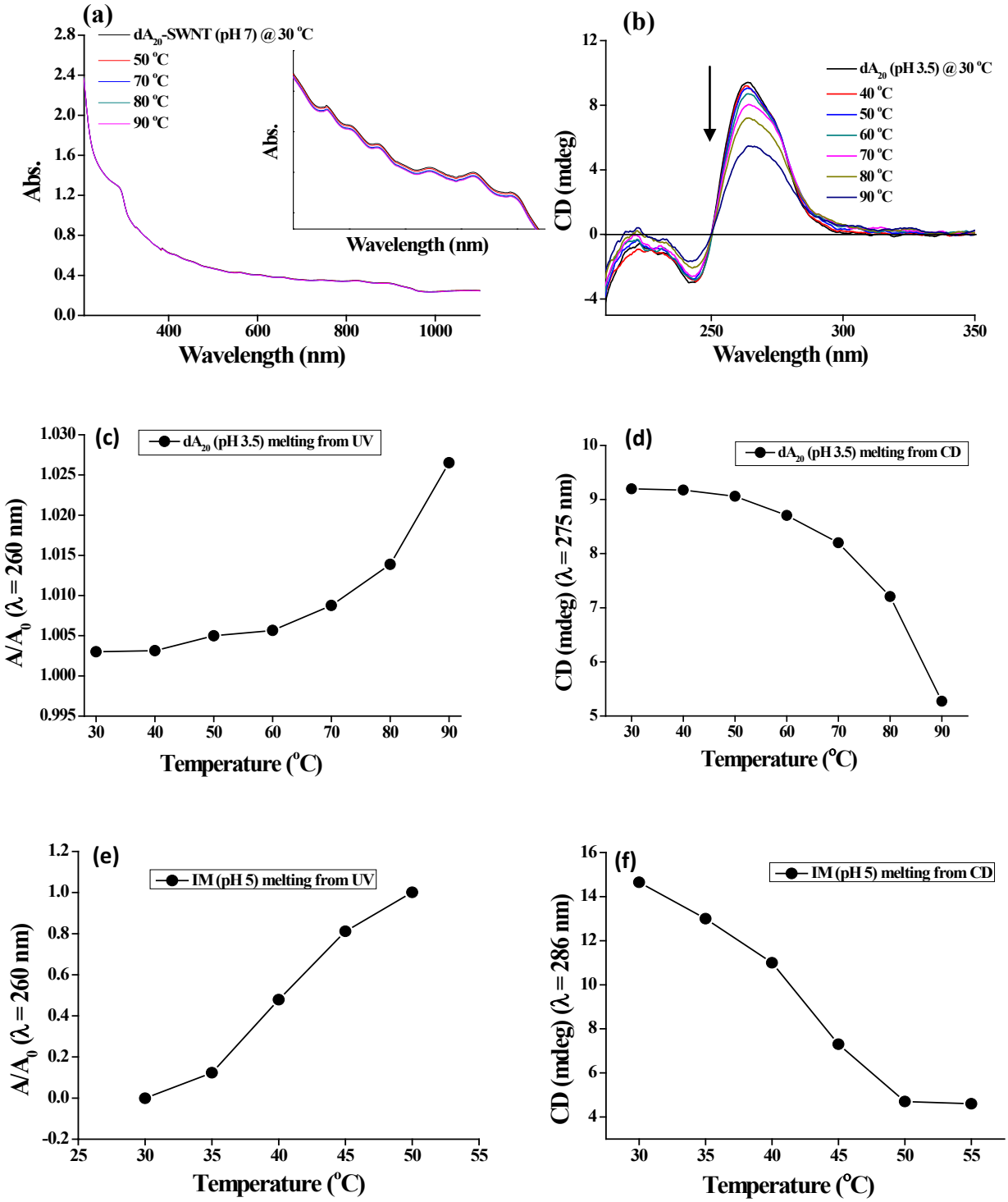

Figure S11. (a) Variable temperature UV-Vis spectra of dA_{20}-SWNT complex solution at pH 7. (b) Variable temperature CD spectra of dA_{20} at pH 3.5 obtained upon acidification of dA_{20}-SWNT complex and (d) the corresponding melting profile. (c) UV melting profile of dA_{20} at pH 3.5 obtained upon acidification of dA_{20}-SWNT complexes at 260 nm. (e,f) UV and CD melting profile of IM at pH 5.0 obtained upon acidification of IM-SWNT complexes.

Laser irradiation of DNA-SWNT complex

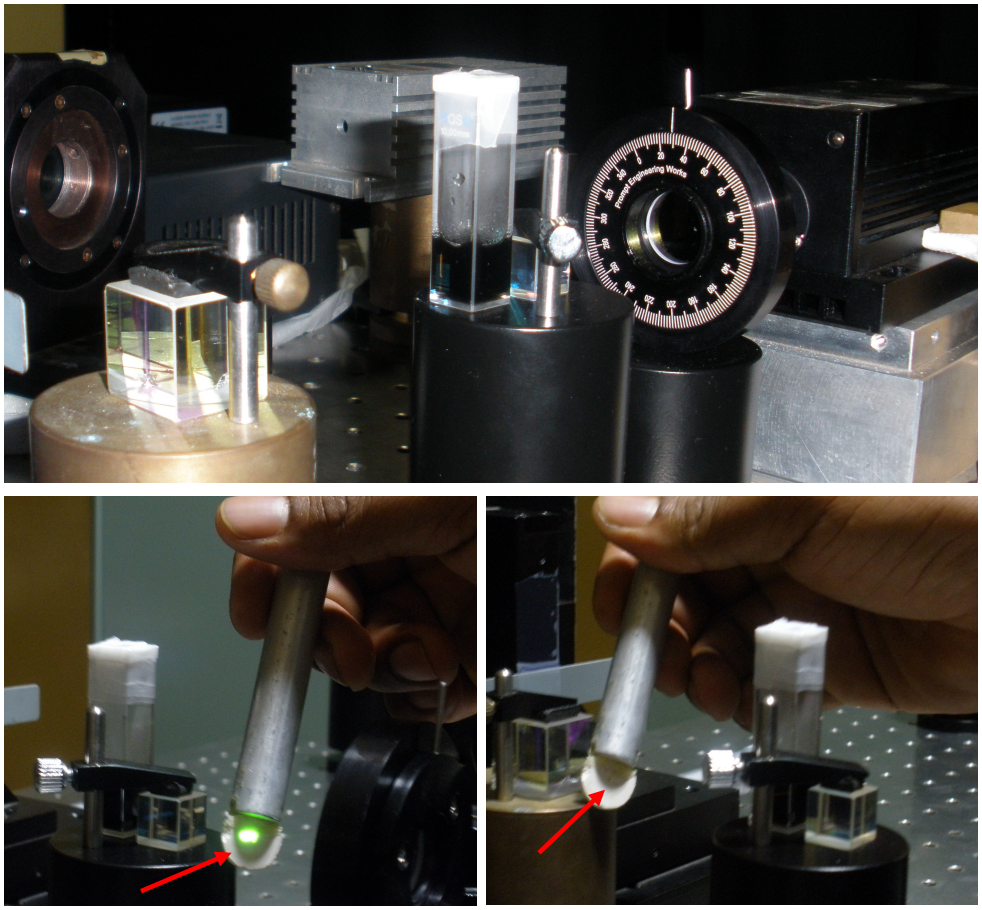

Figure S12. (Top) setup for laser irradiation of DNA-SWNT complex dispersion in water. (Below) ZnO indicator showing intensity of the laser beam before and after passing through the sample. It appears that no laser beam emanating out of the sample suggesting nearly total absorption of the NIR radiation by the sample.

Laser irradiation of DNA-SWNT complex

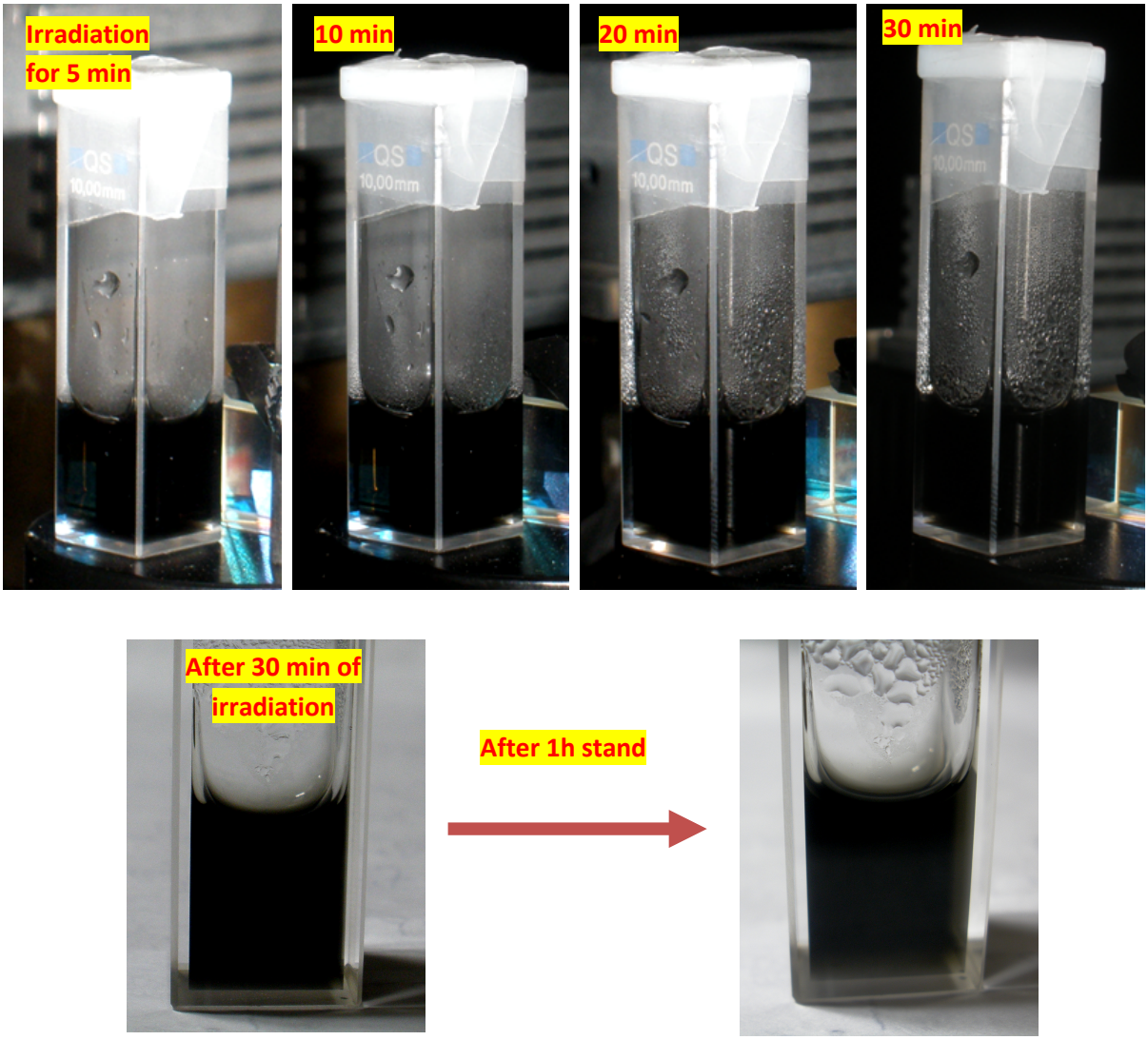

Figure S13. (Top) Photographs showing aqueous suspension of DNA-SWNT complexes which have been exposed to 1064 nm broadband laser radiation for various period of time. The condensation of water vapour on the top of the cuvette surface clearly indicates the heating of the sample upon irradiation. (Below) Photographs showing the stability of the dispersion even after 1h stand of the irradiated sample.

Possible interactions between DNA-SWNT and DNA-DNA at different pH

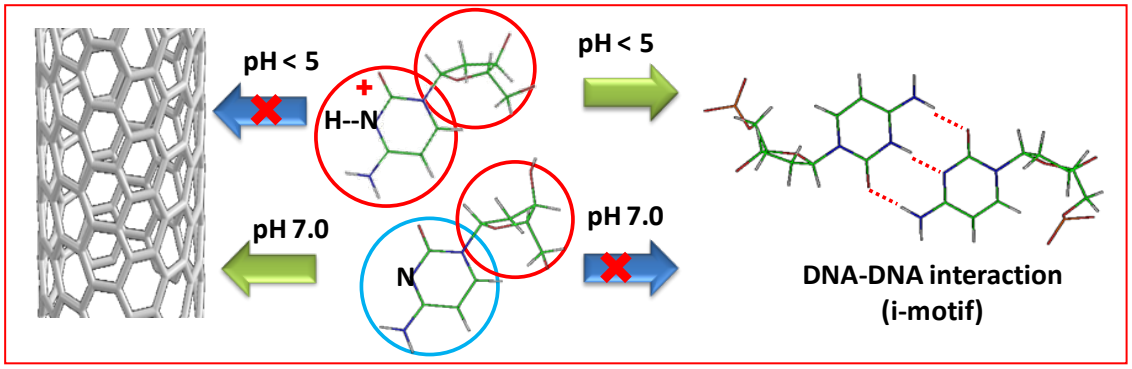

Figure S14. Schematic representation of the various possible interactions between DNA-SWNT and DNA-DNA at different pH of the medium. Blue circle resembles hydrophobic component and red circle resembles the hydrophilic component in DNA.

Conductivity measurement study

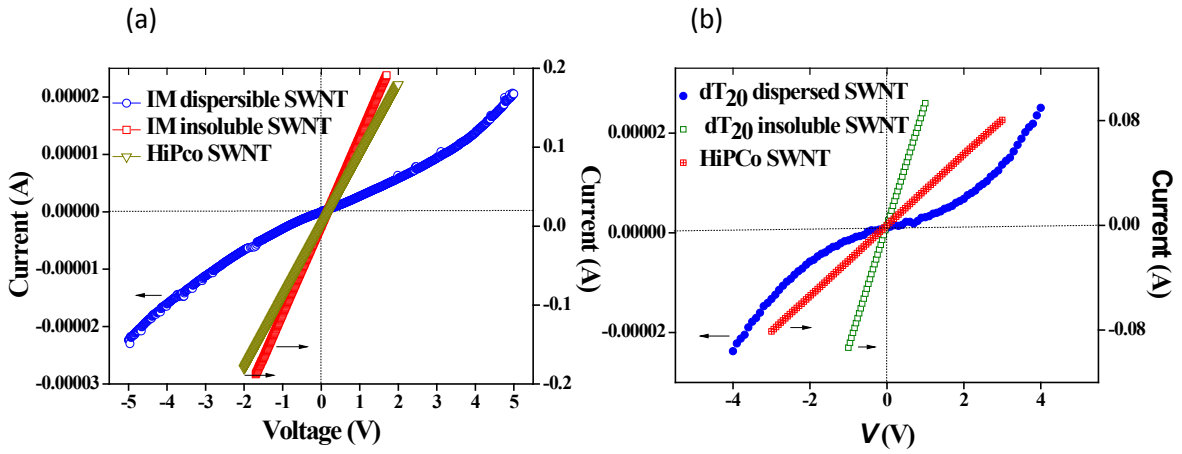

Figure S15. Electrical conductivity (*I-V*) measurements of (a) HiPco SWNT, IM-dispersible SWNT and the IM insoluble SWNT and (b) HiPco SWNT, dT_{20}- dispersible SWNT and the dT_{20} insoluble SWNT in a two-probe electrode.

References.

[I] Y. Wang, H. Shan, R. H. Hauge, M. Pasquali and R. E. Smalley, *J. Phys. Chem. B,* 2007, **111**, 1249-1252.

[II] J.-L, Leroy, M. Gueron, J.-L. Mergny and C. Helene, *Nucleic Acids Res.,* 1994, **22**, 1600-1606.

[III] S. Chakraborty, S. Sharma, P. K. Maiti and Y. Krishnan, *Nucleic Acids Res.,* 2009, **37**, 2810-2817.

[IV] S. Jung, M. Cha, J. Park, N. Jeong, G. Kim, C. Park, J. Ihm and J. Lee, *J. Am. Chem. Soc.,* 2010, **132**, 10964-10966.